SECTION 45

SPECTRAL REFLECTANCE MEASUREMENTS OF A VIRUS HOST MODEL

by

Robert W. Toler, Associate Professor
Department of Plant Sciences
Remote Sensing Center
Texas A&M University
College Station, Texas 77843

N. K. Shankar, Staff Engineer
Lockheed Electronics Co.
Houston, Texas

INTRODUCTION

Insects, weeds, and diseases are hazards to crop production and must be managed. Plant protection is designed for reduction of these crop pests, in order to provide our society with food, fiber, oils and ornamentals while preserving a wholesome environment. Plant diseases are caused by bacteria, fungi, nematodes, phanerogams (parasitic seed plants), mycoplasma, and viruses; viruses incite diseases that limit production of the major food crops of the world. The plant viruses and mycoplasma in most host translocate to the growing point of the plant. Viruses are obligate parasites and multiply only in living cells. A few examples are: Maize Dwarf Mosaic Virus which causes losses in corn, sorghum, and millet; Wheat Streak Mosaic Virus reduces production of wheat, oats, and barley; Barley Yellow Dwarf Virus invades barley, wheat, and oats; Sugarcane Mosaic Virus lowers yield of sugarcane, sorghum, and corn; Tungro or Yellow Orange Leaf Virus is one of the most serious diseases of rice in Asia today and Hoja Blanca Virus attacks rice here in the western hemisphere; and Coconut Lethal Yellowing has destroyed coconut plantings in Jamaica and Florida. Disease management programs to be used effectively in intergrated systems for controlling all pests on a crop will require new disease survey techniques.

This research was a cooperative effort of the Department of Plant Sciences College of Agriculture, Remote Sensing Center, Texas A&M University, College Station, Texas (supported by NASA Grant NsG 239-62) and NASA/MSC/EOD, Applied Physics Branch, Houston, Texas. Valuable assistance was provided by Dr. Forrest Hall,

physicist, Applied Physics Branch NASA/MSC/EOD, Houston; Mr. E. H. Krauss, supervisor, and Mr. Jack Hartman, photoscientist, Lockheed Electronics, Inc., Houston Aerospace Systems Division Photo-optical Science Section NASA/MSC/Houston; and Mr. William Odle, Graduate Assistant, Department of Plant Sciences, Texas A&M University, College Station, Texas.

Virus-host Model

St. Augustinegrass (Stenotaphrum secundatum), the host of St. Augustine Decline, was selected as a disease model to study spectral reflectance properties in order to differentiate healthy from infected grass by remote sensing techniques. In this disease-host combination the host was selected because it is 1) a monocot, 2) produces turf, 3) perennial in nature, 4) vegetatively propagated, 5) genetically stable, 6) adapted to the test site environment, 7) the disease reaction is a typical mosaic, and 8) susceptible to mechanical transmission. The incubation period of the disease is 21-30 days transmitted mechanically, and has a limited host range that includes crabgrass, millet, and St. Augustinegrass.

The experiment discussed here is the multispectral tone signatures of the St. Augustine Decline diseased and healthy targets. Two objectives were: 1) to predict theoretical tone values of healthy and infected St. Augustinegrass on various film/filter/polarization combinations, using spectrometric measurements of light reflectance, film sensitivity data, and filter transmittance curves; 2) to measure the correlation between theoretical tone values and actual tone values as obtained by densitometric analysis of photo negatives. From this information multispectral tone signatures of the healthy and infected St. Augustinegrass can be determined, and optimum film/filter combinations to be used in multispectral photography can be selected.

PROCEDURE

Plant material for laboratory and field studies employed both mechanically inoculated and naturally infected grass showing varying levels of disease development. The split plot technique was used in our field trials with the healthy controls and St. Augustine Decline diseased grass. The plot size was 8 x 8 ft. replicated 12 times (Figure 1). Mechanical inoculations were made in the greenhouse using 600 mesh carborundum and phosphate buffer pH 7.5, .01 M. Inoculum was diseased leaf tissue and buffer at a 1:1 ratio by

weight, ground in a mortar with 1 percent carborundum. Data acquisition included: 1) measuring the spectral reflectance of samples in the laboratory, using the Cary-14 RI spectrophotometer, 2) measuring the spectral reflectance of field plots, using field instruments such as the EG&G spectroradiometer, 3) photographing laboratory samples and field plots, using multiband photographic sensors with various film/filter/polarization combinations, and 4) performing polarization measurements in the laboratory, using a modified Cary-14 RI spectrogoniophotometer.

Cary-14 RI Laboratory Data Acquisition

The model - 14 RI spectrophotometer was employed for automatic recording of spectra in the wavelength region of 2,250 Å to 30,000 Å with good resolving power and high photometric accuracy. Interchangeable light sources for the instrument are a hydrogen lamp, a tungsten lamp for the visible region, and a tungsten lamp for the near-infrared region.

Samples of St. Augustinegrass plants were inoculated with virus at various intervals. These plants were kept under controlled greenhouse conditions at Texas A&M University. Grass blades from these plants were cut to size to be placed in the sample cup of the reflectometer. Various orientations of the grass blades in the sample cup were used to measure the diffuse spectral reflection function in the wavelength region of 350 to 900 nm. Similar measurements were made on the healthy grass samples. The effects of background on the samples were also explored (Figure 2).

Spectral reflectance curves obtained from Cary-14 are shown in Figures 3 and 4.

Multiband Photography

An array of four Nikon-F cameras was mounted on a specially made frame (Figure 5). This frame was then mounted on a tropod stand. Each camera was boresighted on the target. Field irradiance shutter speed calibration and spectral transmission of each lens/filter combination were performed. Three film/filter combinations were selected. Wratten filters 47B, 58, and 25, in combination with black and white plus-X type film, were used in taking spectral multiband photographs of healthy and infected St. Augustinegrass plants, in daylight at various sun angles and in photoflood light under indoor

lighting conditions. Black and white IR, color IR, and Ektrachrome color photographs were also made. Very good correlation between Cary-14 data and photographic density was observed. The results are shown in Figures 6 and 7.

The Nikon camera array was used in the multiband photography of control plots and field work. A cherry picker crane was used to hoist the equipment 35 to 45 ft. above the ground.

Polarization Spectral Reflectance Measurements

The polarization spectral reflectance of grass samples was measured using a modified Cary-14 RI spectrophotometer with a Cary model 50-400-000 gonioreflectometer. The instrument was modified to accept an externally mounted RCA C31034D GaInAs photomultiplier tube and FET-preamp. The Cary gonioreflectometer employs a 25-cm diameter integrating sphere with a tiltable sample holder in the center of the sphere. The sphere is illuminated with undispersed light from a 1,000-W quartz-iodine lamp. A 5-cm quartz lens mounted in the bottom of the sphere projects the image of the lamp filament on the underside of the sample holder. The measurements of the vertical and horizontal polarization components of the reflected light was accomplished by positioning two 3-cm aperture Glan-Thompson prisms in the two sample cell holders located in the sample cell compartment. The reflectance data, 0 percent, 10 percent maximum, and 100 percent of the two components, were recorded on punched paper tape, using the Datex model CU-702-0 data logger. Polarization spectra of healthy and infected grass samples were measured and recorded on the paper tape. This tape was fed into a time-sharing terminal of an XDS Sigma 7 computer. The data was edited, translated, normalized, and reduced to give average reflectance and percent polarization. Polarization values from +100 percent to -100 percent were plotted on an X-Y recorder (Figure 5). Individual perpendicular and parallel polarization components and average values were also plotted. Polarizing filters in conjunction with spectral bandpass filters were used on the Nikon camera systems to record multispectral photographic data.

Spectroradiometer Measurements

The model 580/585 EG&G spectroradiometer system, consisting of a 580-11A indicator unit, a 580-20A series detector head, 585-30 series beam input optics, 585-11 monochromator housings with proper gratings

of the 580-20 series, and other accessories, was used for measuring the spectral reflectance power of healthy and infected St. Augustinegrass plots in the field. The input optical unit mounted along with the monochromator unit and detector head, on a tripod mount, was pointed toward the target. Monochromator slits were adjusted to the calibrated settings. Current output of the detector for each wavelength setting was monitored on the indicator unit and recorded. Prefilters were used to eliminate the high-order interference. A standard white reference target was placed in front of the sensing unit, and spectral reflectance values were measured at the same lighting conditions. The ratios of currents of sample grass to white reference at all wavelengths were calculated. One sample of such experimental data is presented in Figure 8. The hemispherical flux input received at the ground level was measured using an ISCO radiometer. These data were used to apply corrections to EG&G data.

RESULTS AND DISCUSSION

Spectral reflectance data from the Cary-14 RI spectrophotometer showed spectral differences between healthy and diseased plants. Ten to 15 percent differences were found in the 450 to 480 nm (blue) region, the 550 to 560 nm (yellow green) region, and the 670 to 680 nm (red) region. Variations in the dominant peak wavelength were observed. These differences were also observed in the field data taken with the EG&G spectroraiometer. Polarization measurements indicated major spectral differences between healthy and infected plants; as much as 34 percent difference in reflectance in the 450 to 480 nm region and 40 percent difference in the 670 to 680 nm region. Very little difference was observed in the 540 to 550 nm region.

Qualitative measurements from photographs of plants in the blue and red regions with polarization show that light reflected from healthy plants is more strongly polarized than that from diseased plants. Photographs taken through the blue Wratten 47 filter in conjunction with a polarizer show an excellent differentiation. A large photographic difference also appears in the red region (filter 25 and polarizer combination). Much smaller differences were noted in the 540 to 550 nm region. Although the intensity in the near-IR region (750 to 1,200 nm) is much higher than the visible region of the spectrum, differences in the healthy and diseased plants' reflectance were quite small. A maximum of 10 percent difference was observed in the spectra obtained with the

Cary-14 RI spectrophotometer. Near-IR photographs taken with color IR and black and white IR films showed relatively small tone change between the healthy and infected grass plots.

Black and white negatives of the control plots taken with red, green, and blue filters plus polarizers were analyzed using color density contouring and slicing techniques. A multiband TV display unit manufactured by the IIS Corporation was used for this purpose. The results are shown in Figures 9 and 10. Ratioing densities of the green region to the red region, and the green region to the blue region were attempted using the IIS Corporation imaging system. The results are shown in Figures 11 and 12. There seems to be good correlation between the laboratory results and field data. The healthy grass consistently exhibited a darker image on the negative compared to the diseased grass.

An analysis of results using absolute reflected energy levels will be made in the future work schedule. Modeling for aircraft operation is also contemplated in this schedule. With time progression data acquisition, effective previsual analysis prediction will be attempted.

In conclusion, a technique has been developed to detect the characteristic spectral signature of healthy and infected St. Augustinegrass. It is possible to predict the coverage of the infected area provided ground truth coverage shows positive St. Augustinegrass turf. Positive identification of healthy and diseased grass is attempted, but no attempt has been made to isolate the virus symptoms from any other symptoms or effects.

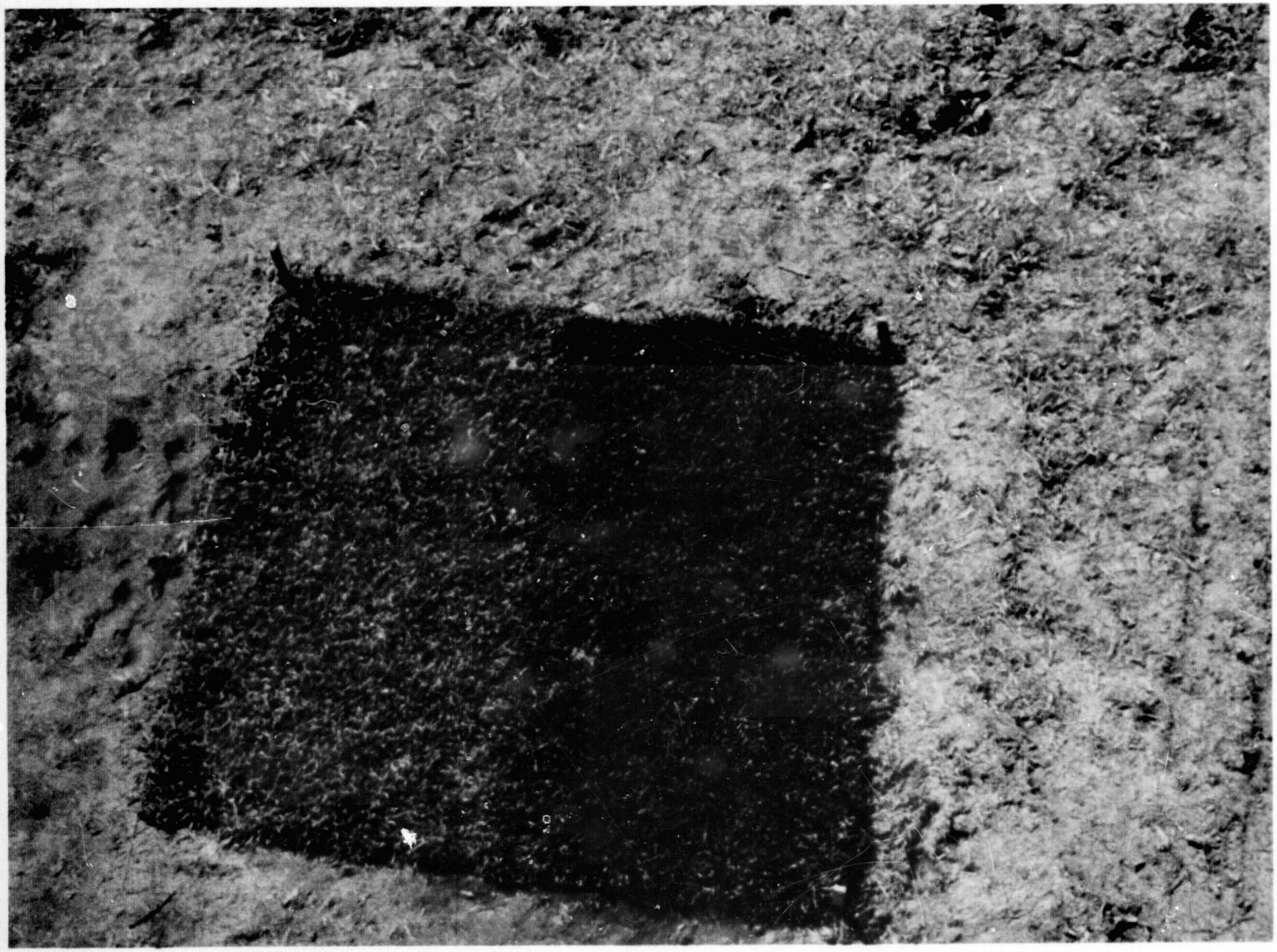

Figure 1. Field plot 8 x 8 ft. split 4 x 8 ft. healthy grass and 4 x 8 ft. St. Augustine Decline diseased grass.

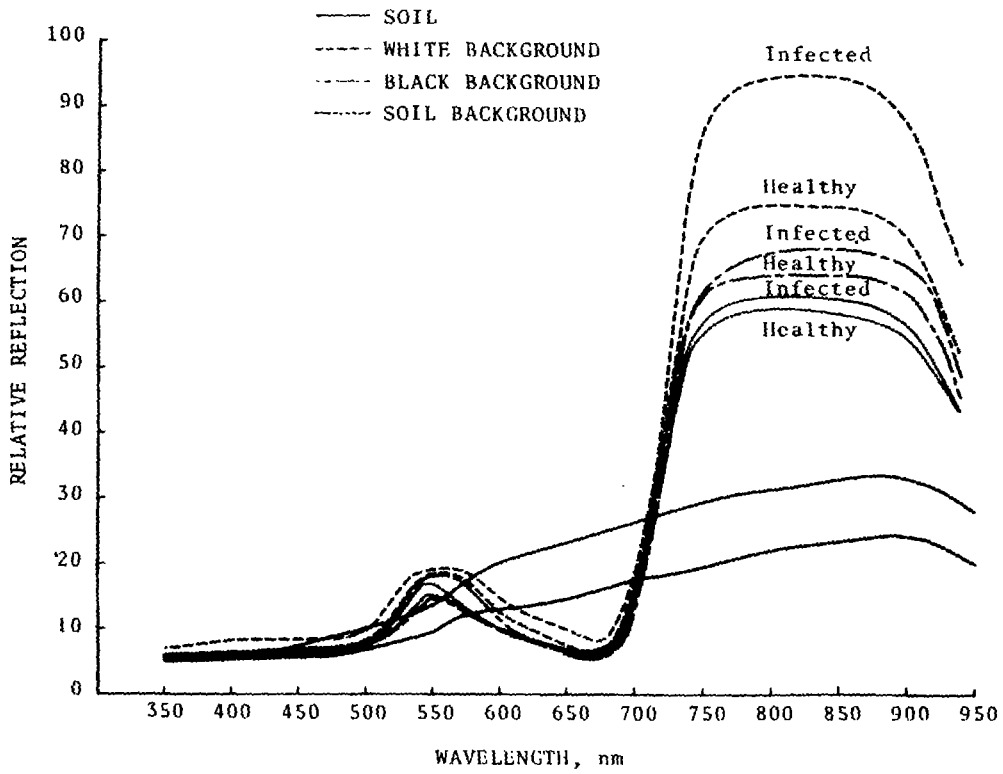
SOIL
WHITE BACKGROUND
BLACK BACKGROUND
SOIL BACKGROUND
Infected
Healthy
Infected
Healthy
Infected
Healthy
RELATIVE REFLECTION
100
90
80
70
60
50
40
30
20
10
0
350
400
450
500
550
600
650
700
750
800
850
900
950
WAVELENGTH, nm

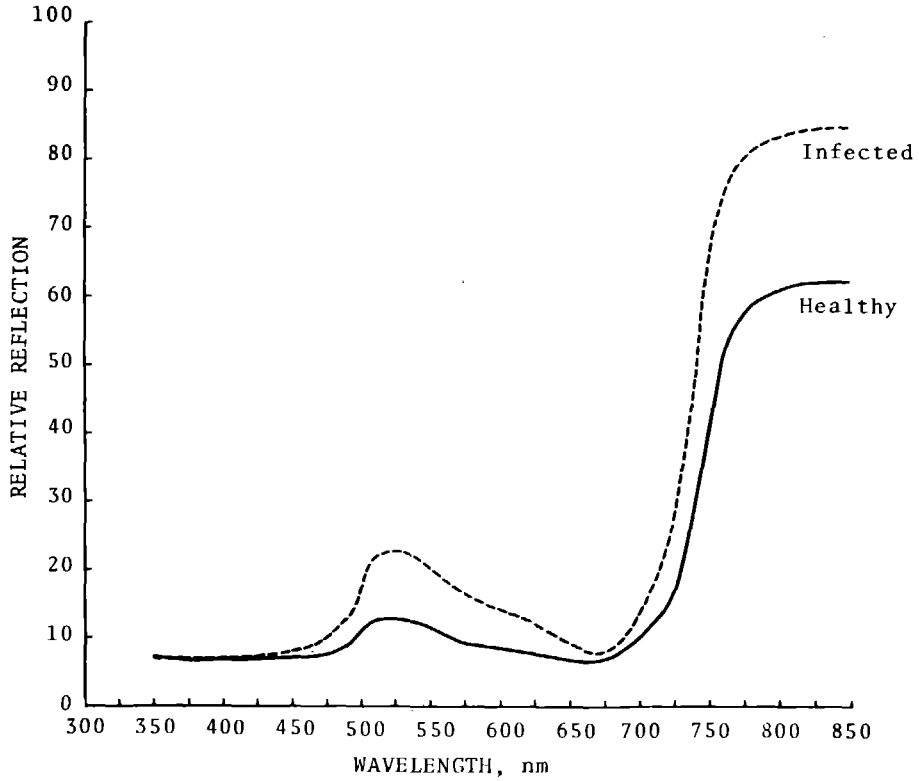

Figure 3. Cary-14 RI spectrophotometer results: reflectance spectra of healthy and infected St. Augustinegrass samples.

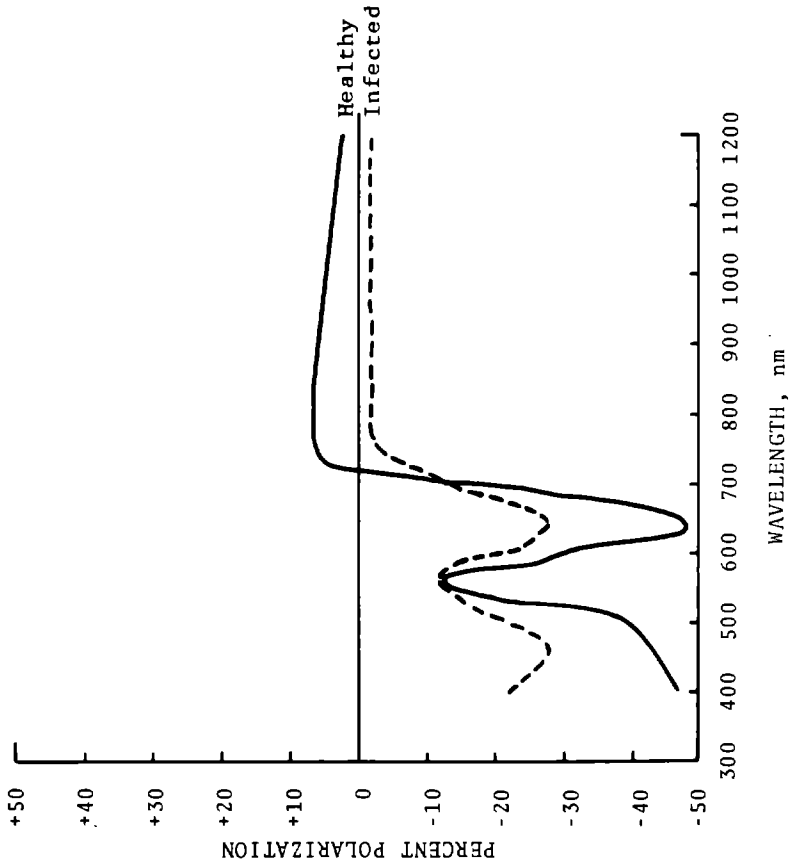

Figure 4. Cary-14 RI spectrophotometer results: polarization reflectance spectra of healthy and infected St. Augustinegrass samples.

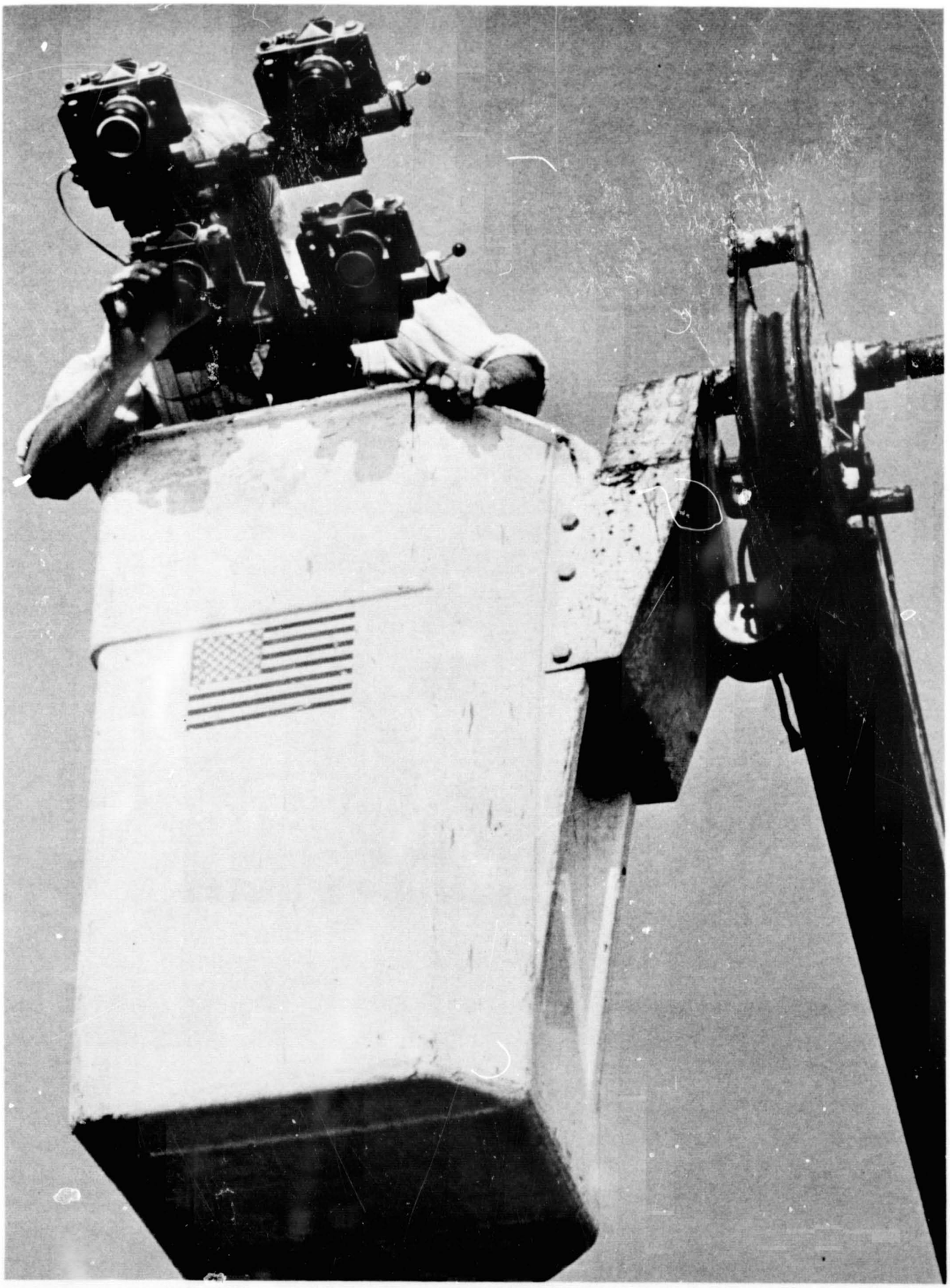

Figure 5. Nikon camera four-band system on the cherry picker crane.

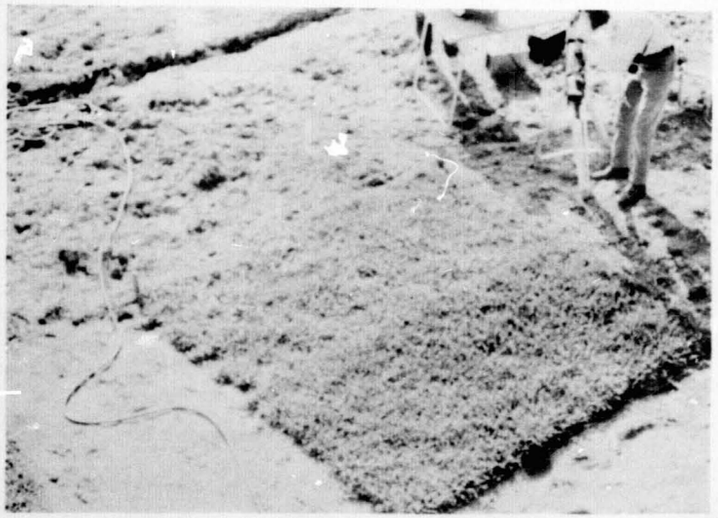

Wratten 25 (red)

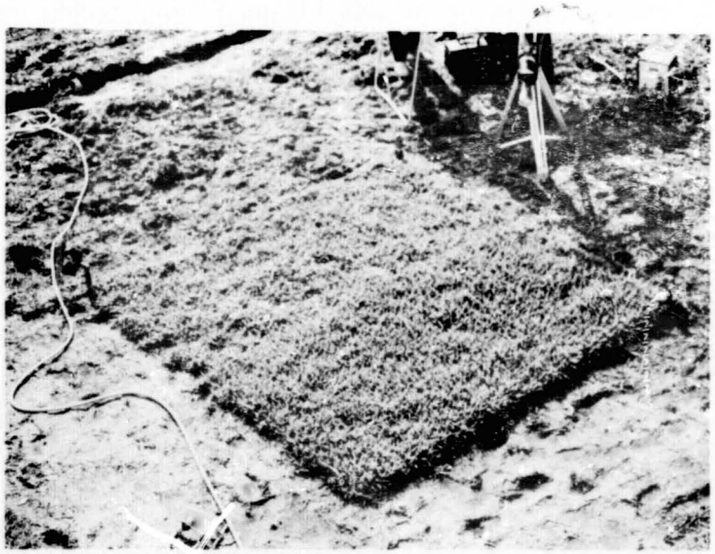

Wratten 58 (green)

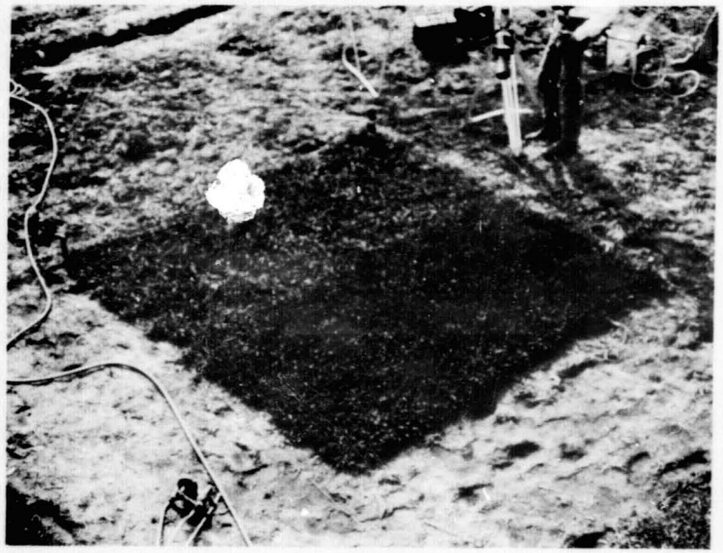

Wratten 47B (blue)

Figure 6. Field plot photographed through Wratten 25, Wratten 58, and Wratten 47B filters.

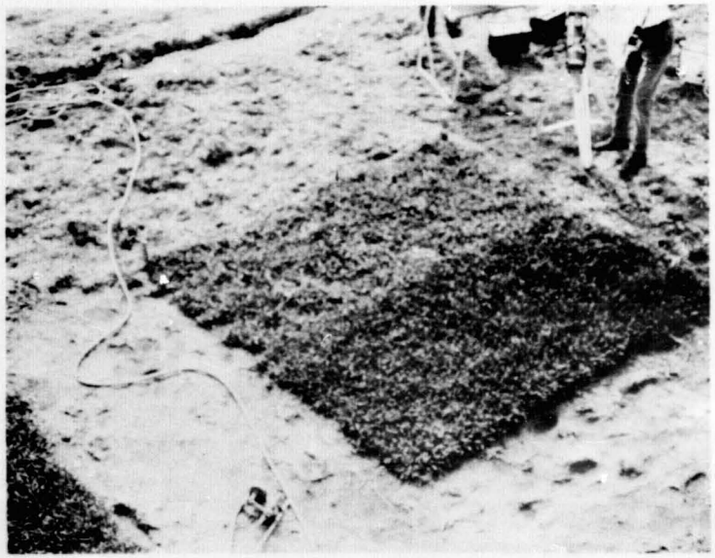

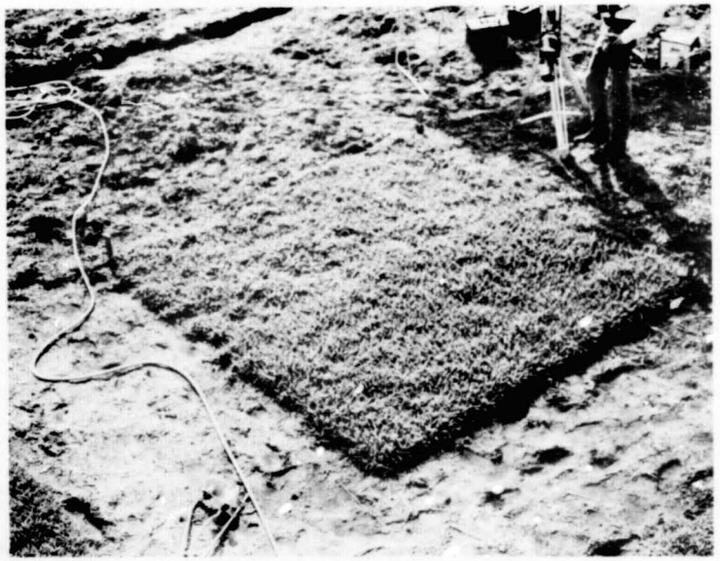

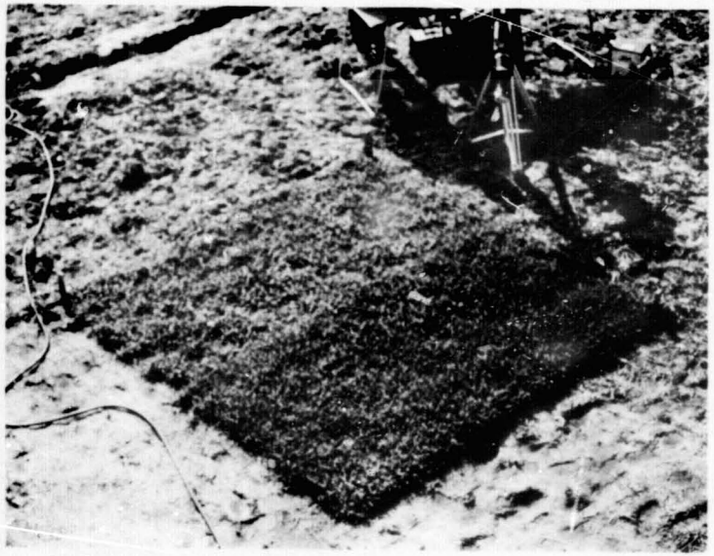

Figure 7. Field plot photographed through Wratten 25 and polarizer, Wratten 58 and polarizer, and Wratten 57B and polarizer.

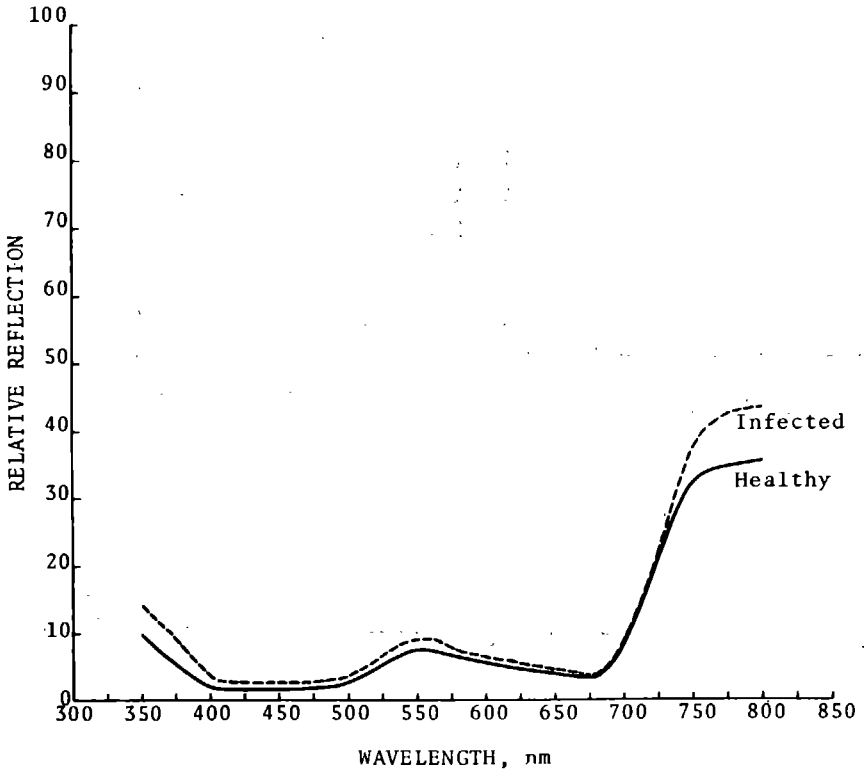

Figure 8. EG&G field measurement results: reflectance spectra of healthy and infected St. Augustinegrass samples.

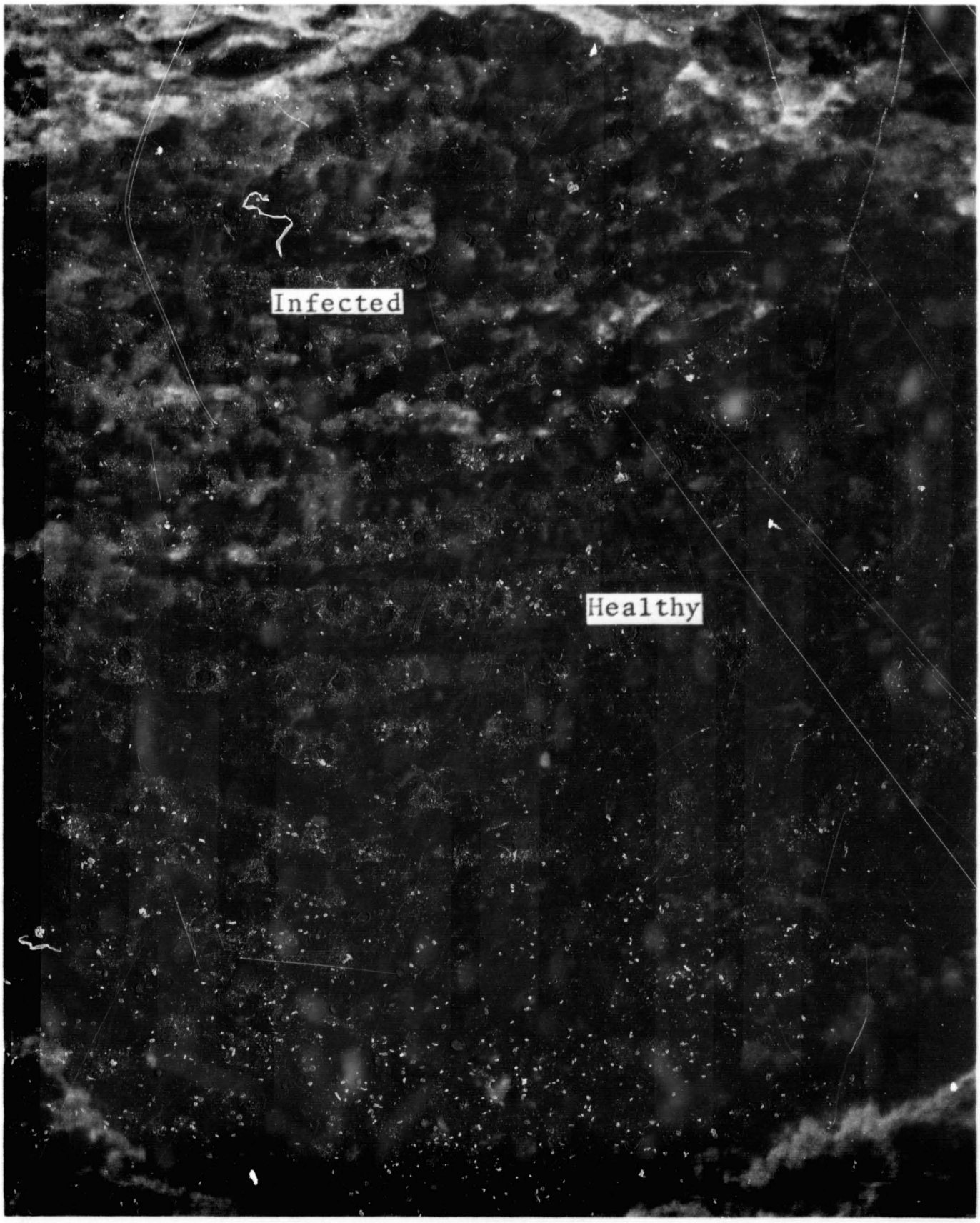

Figure 9. Color density photo of I^2S system photograph of the projection screen. (Red filter and polarizer)

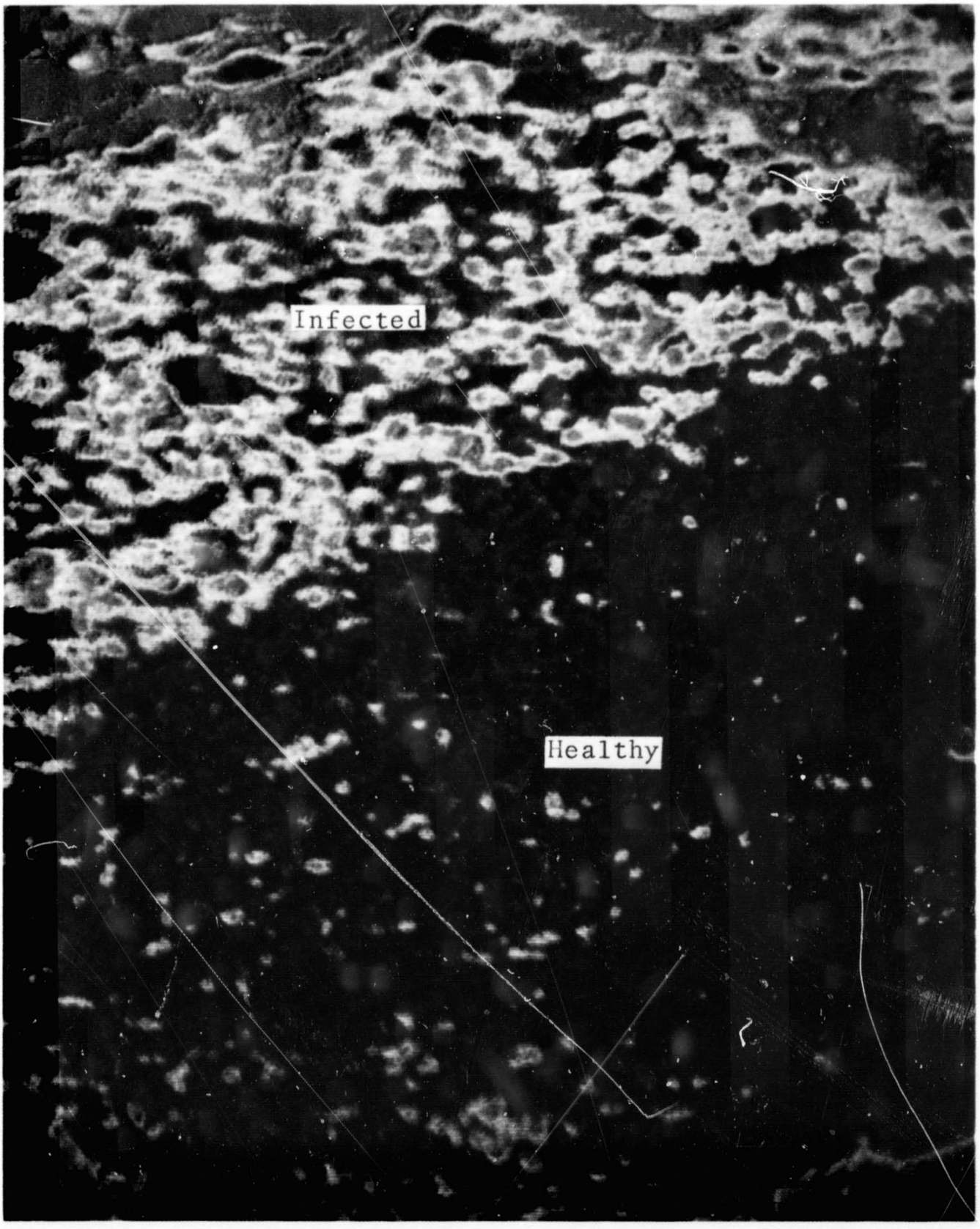

Figure 10. Color density photo of I^2S system photograph of the projection screen (blue filter and polarizer) (concluded).

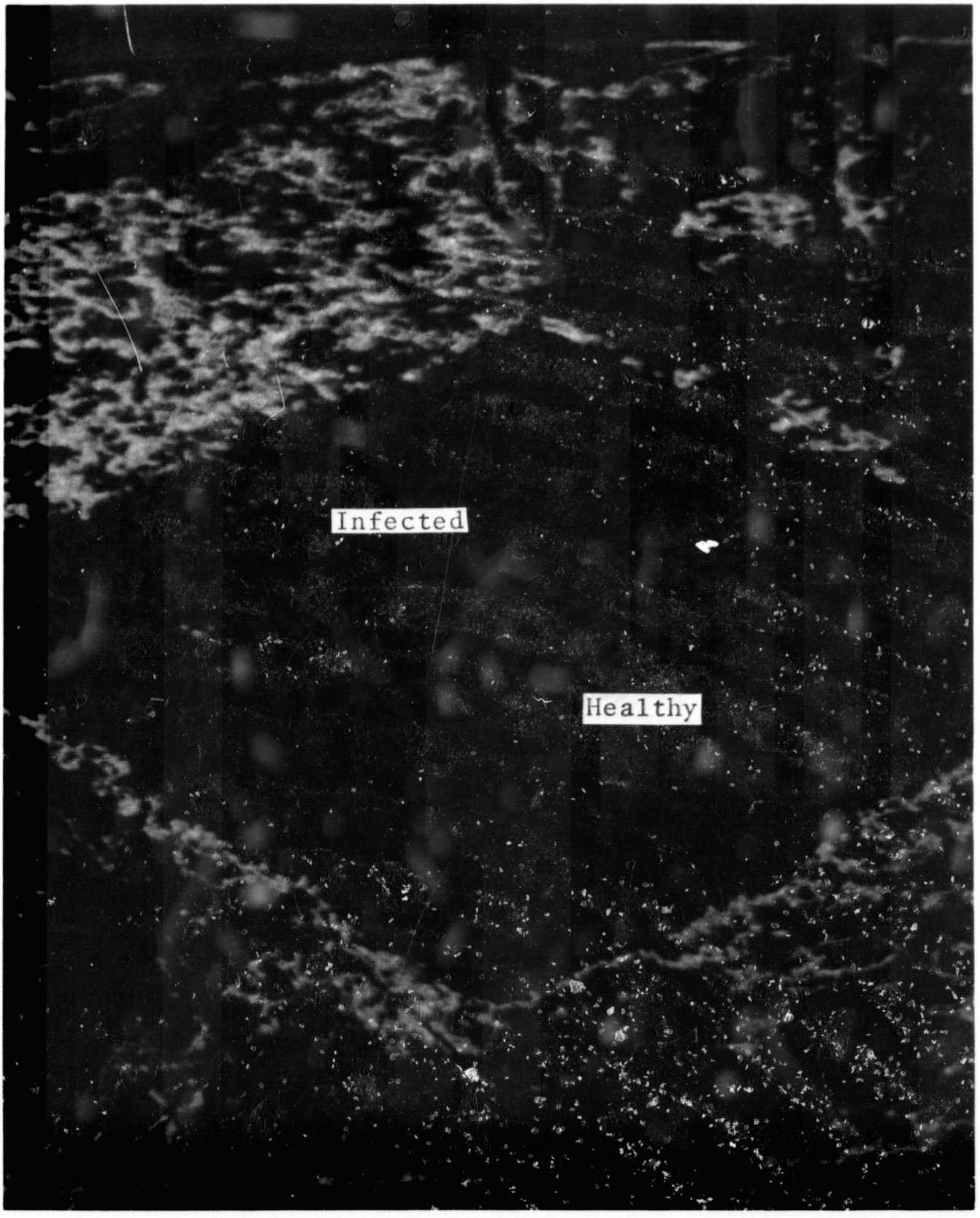

Figure 11. Density discrimination between healthy and infected grass. (Ratio of green density to red density)

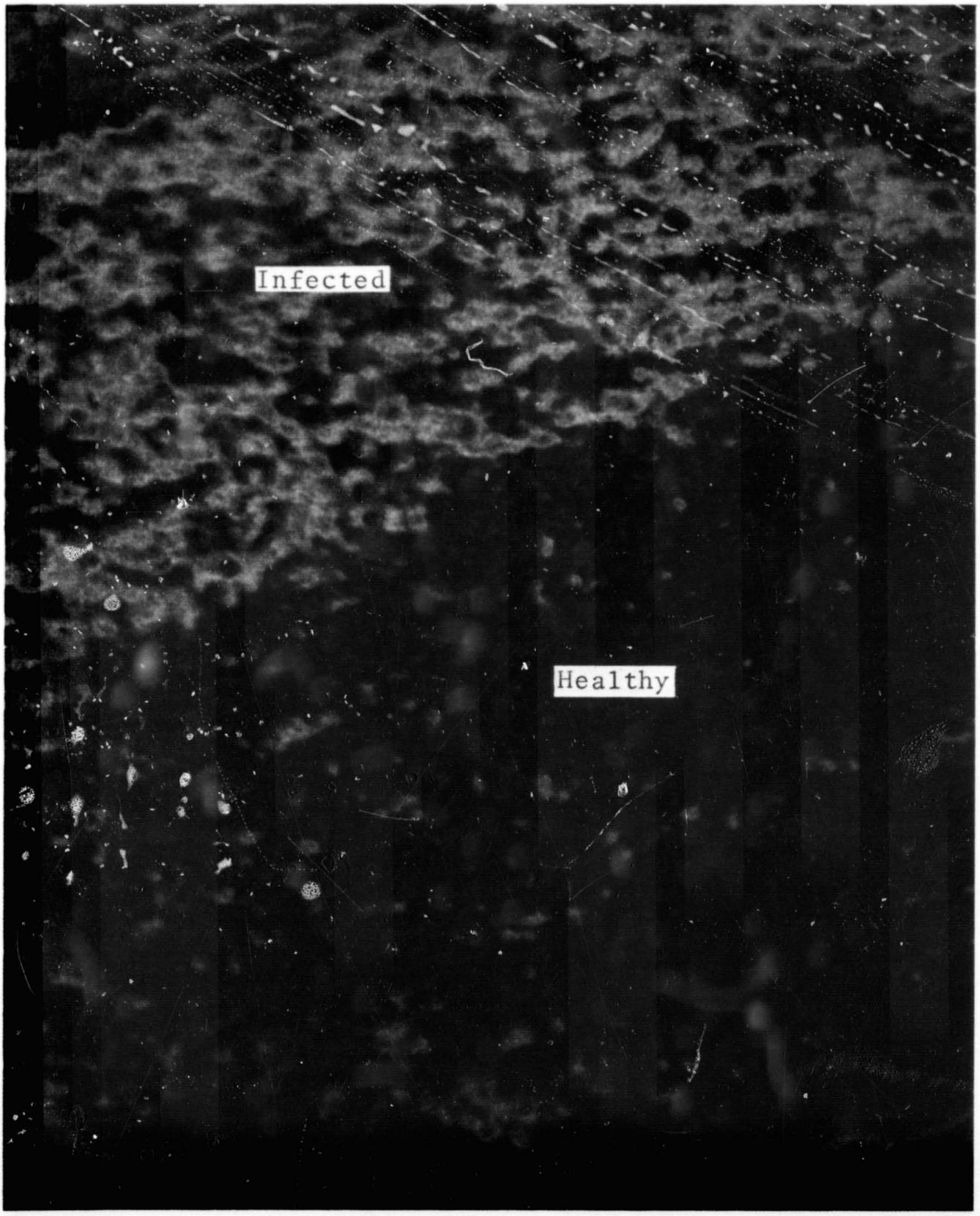

Figure 12. Density discrimination between healthy and infected grass (ratio of green density to blue density) (concluded).